

Search for heavy neutrinos at Belle

D. Liventsev,¹¹ I. Adachi,¹¹ H. Aihara,⁵⁶ K. Arinstein,³ D. M. Asner,⁴⁴ V. Aulchenko,³
T. Aushev,¹⁹ A. M. Bakich,⁵⁰ A. Bay,²⁶ K. Belous,¹⁸ B. Bhuyan,¹⁴ A. Bondar,³
G. Bonvicini,⁶¹ A. Bozek,⁴⁰ M. Bračko,^{29,20} T. E. Browder,¹⁰ P. Chang,³⁹ V. Chekelian,³⁰
A. Chen,³⁷ B. G. Cheon,⁹ R. Chistov,¹⁹ K. Cho,²³ V. Chobanova,³⁰ S.-K. Choi,⁸ Y. Choi,⁴⁹
D. Cinabro,⁶¹ J. Dalseno,^{30,52} Z. Doležal,⁴ Z. Drásal,⁴ A. Drutskoy,^{19,32} D. Dutta,¹⁴
S. Eidelman,³ D. Epifanov,³ S. Esen,⁵ H. Farhat,⁶¹ J. E. Fast,⁴⁴ V. Gaur,⁵¹ N. Gabyshev,³
S. Ganguly,⁶¹ R. Gillard,⁶¹ Y. M. Goh,⁹ B. Golob,^{27,20} J. Haba,¹¹ K. Hayasaka,³⁵
H. Hayashii,³⁶ Y. Horii,³⁵ Y. Hoshi,⁵⁴ W.-S. Hou,³⁹ H. J. Hyun,²⁵ T. Iijima,^{35,34}
A. Ishikawa,⁵⁵ K. Itagaki,⁵⁵ R. Itoh,¹¹ Y. Iwasaki,¹¹ T. Julius,³¹ D. H. Kah,²⁵
J. H. Kang,⁶³ E. Kato,⁵⁵ T. Kawasaki,⁴² C. Kiesling,³⁰ H. J. Kim,²⁵ H. O. Kim,²⁵
J. B. Kim,²⁴ K. T. Kim,²⁴ M. J. Kim,²⁵ Y. J. Kim,²³ J. Klucar,²⁰ B. R. Ko,²⁴
S. Korpar,^{29,20} R. T. Kouzes,⁴⁴ P. Križan,^{27,20} P. Krokovny,³ T. Kuhr,²² R. Kumar,⁴⁵
T. Kumita,⁵⁸ A. Kuzmin,³ Y.-J. Kwon,⁶³ S.-H. Lee,²⁴ J. Li,⁴⁸ Y. Li,⁶⁰ J. Libby,¹⁵ C. Liu,⁴⁷
Y. Liu,⁵ Z. Q. Liu,¹⁶ R. Louvot,²⁶ D. Matvienko,³ K. Miyabayashi,³⁶ H. Miyata,⁴²
R. Mizuk,^{19,32} G. B. Mohanty,⁵¹ A. Moll,^{30,52} N. Muramatsu,⁴⁶ Y. Nagasaka,¹²
E. Nakano,⁴³ M. Nakao,¹¹ Z. Natkaniec,⁴⁰ N. K. Nisar,⁵¹ S. Nishida,¹¹ O. Nitoh,⁵⁹
T. Nozaki,¹¹ S. Ogawa,⁵³ T. Ohshima,³⁴ S. Okuno,²¹ S. L. Olsen,⁴⁸ W. Ostrowicz,⁴⁰
C. Oswald,² P. Pakhlov,^{19,32} G. Pakhlova,¹⁹ H. Park,²⁵ H. K. Park,²⁵ T. K. Pedlar,²⁸
R. Pestotnik,²⁰ M. Petrič,²⁰ L. E. Pilonen,⁶⁰ K. Prothmann,^{30,52} M. Ritter,³⁰
M. Röhrken,²² S. Ryu,⁴⁸ H. Sahoo,¹⁰ T. Saito,⁵⁵ Y. Sakai,¹¹ S. Sandilya,⁵¹ D. Santel,⁵
L. Santelj,²⁰ Y. Sato,⁵⁵ O. Schneider,²⁶ G. Schnell,^{1,13} C. Schwanda,¹⁷ K. Senyo,⁶²
O. Seon,³⁴ M. E. Seviar,³¹ M. Shapkin,¹⁸ C. P. Shen,³⁴ T.-A. Shibata,⁵⁷ J.-G. Shiu,³⁹
B. Shwartz,³ A. Sibidanov,⁵⁰ F. Simon,^{30,52} P. Smerkol,²⁰ Y.-S. Sohn,⁶³ A. Sokolov,¹⁸
E. Solovieva,¹⁹ M. Starič,²⁰ M. Sumihama,⁷ T. Sumiyoshi,⁵⁸ G. Tatishvili,⁴⁴ Y. Teramoto,⁴³
T. Tsuboyama,¹¹ M. Uchida,⁵⁷ S. Uehara,¹¹ T. Uglov,^{19,33} Y. Unno,⁹ S. Uno,¹¹
Y. Ushiroda,¹¹ Y. Usov,³ C. Van Hulse,¹ P. Vanhoefer,³⁰ G. Varner,¹⁰ K. E. Varvell,⁵⁰
V. Vorobyev,³ M. N. Wagner,⁶ C. H. Wang,³⁸ M.-Z. Wang,³⁹ P. Wang,¹⁶ M. Watanabe,⁴²
Y. Watanabe,²¹ K. M. Williams,⁶⁰ E. Won,²⁴ B. D. Yabsley,⁵⁰ H. Yamamoto,⁵⁵
Y. Yamashita,⁴¹ C. C. Zhang,¹⁶ Z. P. Zhang,⁴⁷ V. Zhilich,³ and A. Zupanc²²

(The Belle Collaboration)

¹*University of the Basque Country UPV/EHU, 48080 Bilbao*

²*University of Bonn, 53115 Bonn*

³*Budker Institute of Nuclear Physics SB RAS and
Novosibirsk State University, Novosibirsk 630090*

⁴*Faculty of Mathematics and Physics, Charles University, 121 16 Prague*

⁵*University of Cincinnati, Cincinnati, Ohio 45221*

⁶*Justus-Liebig-Universität Gießen, 35392 Gießen*

⁷*Gifu University, Gifu 501-1193*

⁸*Gyeongsang National University, Chinju 660-701*

⁹*Hanyang University, Seoul 133-791*

- ¹⁰ *University of Hawaii, Honolulu, Hawaii 96822*
- ¹¹ *High Energy Accelerator Research Organization (KEK), Tsukuba 305-0801*
- ¹² *Hiroshima Institute of Technology, Hiroshima 731-5193*
- ¹³ *Ikerbasque, 48011 Bilbao*
- ¹⁴ *Indian Institute of Technology Guwahati, Assam 781039*
- ¹⁵ *Indian Institute of Technology Madras, Chennai 600036*
- ¹⁶ *Institute of High Energy Physics,
Chinese Academy of Sciences, Beijing 100049*
- ¹⁷ *Institute of High Energy Physics, Vienna 1050*
- ¹⁸ *Institute for High Energy Physics, Protvino 142281*
- ¹⁹ *Institute for Theoretical and Experimental Physics, Moscow 117218*
- ²⁰ *J. Stefan Institute, 1000 Ljubljana*
- ²¹ *Kanagawa University, Yokohama 221-8686*
- ²² *Institut für Experimentelle Kernphysik,
Karlsruher Institut für Technologie, 76131 Karlsruhe*
- ²³ *Korea Institute of Science and Technology Information, Daejeon 305-806*
- ²⁴ *Korea University, Seoul 136-713*
- ²⁵ *Kyungpook National University, Daegu 702-701*
- ²⁶ *École Polytechnique Fédérale de Lausanne (EPFL), Lausanne 1015*
- ²⁷ *Faculty of Mathematics and Physics,
University of Ljubljana, 1000 Ljubljana*
- ²⁸ *Luther College, Decorah, Iowa 52101*
- ²⁹ *University of Maribor, 2000 Maribor*
- ³⁰ *Max-Planck-Institut für Physik, 80805 München*
- ³¹ *School of Physics, University of Melbourne, Victoria 3010*
- ³² *Moscow Physical Engineering Institute, Moscow 115409*
- ³³ *Moscow Institute of Physics and Technology, Moscow Region 141700*
- ³⁴ *Graduate School of Science, Nagoya University, Nagoya 464-8602*
- ³⁵ *Kobayashi-Maskawa Institute, Nagoya University, Nagoya 464-8602*
- ³⁶ *Nara Women's University, Nara 630-8506*
- ³⁷ *National Central University, Chung-li 32054*
- ³⁸ *National United University, Miao Li 36003*
- ³⁹ *Department of Physics, National Taiwan University, Taipei 10617*
- ⁴⁰ *H. Niewodniczanski Institute of Nuclear Physics, Krakow 31-342*
- ⁴¹ *Nippon Dental University, Niigata 951-8580*
- ⁴² *Niigata University, Niigata 950-2181*
- ⁴³ *Osaka City University, Osaka 558-8585*
- ⁴⁴ *Pacific Northwest National Laboratory, Richland, Washington 99352*
- ⁴⁵ *Panjab University, Chandigarh 160014*
- ⁴⁶ *Research Center for Electron Photon Science,
Tohoku University, Sendai 980-8578*
- ⁴⁷ *University of Science and Technology of China, Hefei 230026*
- ⁴⁸ *Seoul National University, Seoul 151-742*
- ⁴⁹ *Sungkyunkwan University, Suwon 440-746*
- ⁵⁰ *School of Physics, University of Sydney, NSW 2006*
- ⁵¹ *Tata Institute of Fundamental Research, Mumbai 400005*
- ⁵² *Excellence Cluster Universe, Technische Universität München, 85748 Garching*

⁵³*Toho University, Funabashi 274-8510*

⁵⁴*Tohoku Gakuin University, Tagajo 985-8537*

⁵⁵*Tohoku University, Sendai 980-8578*

⁵⁶*Department of Physics, University of Tokyo, Tokyo 113-0033*

⁵⁷*Tokyo Institute of Technology, Tokyo 152-8550*

⁵⁸*Tokyo Metropolitan University, Tokyo 192-0397*

⁵⁹*Tokyo University of Agriculture and Technology, Tokyo 184-8588*

⁶⁰*CNP, Virginia Polytechnic Institute and State University, Blacksburg, Virginia 24061*

⁶¹*Wayne State University, Detroit, Michigan 48202*

⁶²*Yamagata University, Yamagata 990-8560*

⁶³*Yonsei University, Seoul 120-749*

(Dated: October 29, 2018)

Abstract

We report on a search for heavy neutrinos in B -meson decays. The results are obtained using a data sample that contains $772 \times 10^6 B\bar{B}$ pairs collected at the $\Upsilon(4S)$ resonance with the Belle detector at the KEKB asymmetric-energy e^+e^- collider. No signal is observed and upper limits are set on mixing of heavy neutrinos with left-handed neutrinos of the Standard Model in the mass range $0.5 \text{ GeV}/c^2 - 5.0 \text{ GeV}/c^2$.

PACS numbers: 12.60.-i,13.35.Hb,14.60.Pq

The masses of particles in the Standard Model (SM) are generated by the coupling of the Higgs field to the left- and right-handed components of a given particle. There being no right-handed neutrino components in the SM, neutrinos in the SM are strictly massless. However, experimental data on neutrino oscillations show that neutrinos are not massless, though their masses are very small [1]. Therefore, a mechanism beyond the SM is needed to establish neutrino masses. One possibility is the addition of right-handed neutrinos, which may also have a Majorana mass, naturally explaining the smallness of the observed neutrino masses via the so-called “see-saw” mechanism [2]. For example, the neutrino minimal Standard Model (ν MSSM) [3] introduces three right-handed singlet heavy neutrinos, so that every left-handed particle has a right-handed counterpart. This model explains neutrino oscillations, the existence of dark matter and baryogenesis with the same set of parameters. Heavy neutrinos also appear in other extensions to the SM, such as SUSY [4], grand unification theories [5] or models with exotic Higgs representations [6].

In general, neutrino flavor eigenstates need not coincide with the mass eigenstates but may be related through a unitary transformation, similar to the one that applies to the quark sector,

$$\nu_\alpha = \sum_i U_{\alpha i} \nu_i, \quad \alpha = e, \mu, \tau, \dots, \quad i = 1, 2, 3, 4, \dots \quad (1)$$

where α denotes the flavor eigenstates and i denotes the mass eigenstates. Production and decay diagrams for heavy neutrinos are shown in Fig. 1. The coupling of the heavy neutrino ν_4 to the charged current of flavor α is characterized by a quantity $U_{\alpha 4}$. Below, we denote a heavy neutrino in the mass range accessible at Belle and its corresponding coupling constant by ν_h and U_α , respectively. Existing experimental results are reviewed and discussed in Ref. [7].

In this paper, we describe a direct search for heavy neutrino decays $\nu_h \rightarrow \ell^\pm \pi^\mp$, $\ell = e, \mu$ with the Belle detector. The measurement is based on a data sample that contains 772 million $B\bar{B}$ pairs, which corresponds to 711 fb^{-1} , collected at the $\Upsilon(4S)$ resonance with the Belle detector operating at the KEKB asymmetric-energy e^+e^- collider [8]. The Belle detector is a large-solid-angle magnetic spectrometer that consists of a silicon vertex detector (SVD), a 50-layer central drift chamber (CDC), an array of aerogel threshold Cherenkov counters (ACC), a barrel-like arrangement of time-of-flight scintillation counters (TOF), and an electromagnetic calorimeter comprised of CsI(Tl) crystals (ECL) located inside a superconducting solenoid coil that provides a 1.5 T magnetic field. An iron flux return located outside the coil is instrumented to detect K_L^0 mesons and to identify muons (KLM). The detector is described in detail elsewhere [9]. Tracking at Belle is done using the SVD and CDC.

Backgrounds are studied using Monte Carlo (MC) samples of known $B\bar{B}$ decays from $b \rightarrow c$ processes (generic MC) that have three times the statistics of the Belle dataset. Signal MC samples of 500,000 events each for different heavy neutrino masses and production mechanisms are used to evaluate the response of the detector, determine its acceptance and efficiency, and optimize selection criteria. Events are generated using the EvtGen program [10]. Heavy neutrinos are produced and decayed using a phase space model.

At Belle, the most favorable mass range to look for a heavy neutrino is $M(K) < M(\nu_h) < M(B)$ [11]. This analysis uses the leptonic and semileptonic B meson decays $B \rightarrow X \ell \nu_h$, where $\ell = e, \mu$ and X may be a charm meson $D^{(*)}$, a light meson (π, ρ, η , etc.) or ‘nothing’ (purely leptonic decay), with relative rates as given in Ref. [11].

A distinctive feature of the heavy neutrino is its long expected flight length: for $M(\nu_h) =$

1 GeV/c² and $|U_e|^2 = |U_\mu|^2 = 10^{-4}$ the flight length is $c\tau \simeq 20$ m. Therefore, the expected overall reconstruction efficiency is small. To improve sensitivity, a partial reconstruction technique is used. A candidate is formed from two leptons and a pion ($\ell_2\ell_1\pi$), where ℓ_1 and π have opposite charge and form the heavy neutrino candidate with a vertex displaced from the interaction point (IP). The lepton ℓ_1 is referred to as the ‘signal lepton,’ while the lepton ℓ_2 , which comes from the B decay, is referred to as the ‘production lepton.’ In this analysis, the heavy neutrino is assumed to be a Majorana fermion and may decay to a lepton of any charge regardless of the original B -meson flavor. If the heavy neutrino were a Dirac fermion, the production and decay leptons would necessarily have opposite charge.

If the heavy neutrino is light enough to be produced via $B \rightarrow D^{(*)}\ell\nu_h$, these production modes are expected to dominate over decays to light mesons due to the small value of the ratio of the relevant CKM matrix elements $|V_{ub}|/|V_{cb}|$. The background is more severe for smaller heavy neutrino masses, $M(\nu_h) < 2$ GeV/c², so an analysis using only $B \rightarrow D^{(*)}\ell\nu_h$ modes is used in this “small mass” regime, while the full inclusive analysis is used in the “large mass” regime.

To suppress the QED background, the charged multiplicity in the event is required to be larger than four. Charged tracks positively identified as electrons or muons (as defined in the next paragraph) with laboratory-frame momentum greater than 0.5 GeV/c are used as leptons. All other tracks in the event are treated as pion candidates. Additional selection criteria for the lepton and pion tracks are described below.

A significant background remains for heavy neutrino candidates from particles with similar event topology, notably $K_S^0 \rightarrow \pi^+\pi^-$, $\Lambda \rightarrow p\pi^-$, $\gamma \rightarrow e^+e^-$. These backgrounds are suppressed by strict lepton identification requirements. Electrons are identified using the energy and shower profile in the ECL, the light yield in the ACC and the specific ionization energy loss in the CDC (dE/dx). This information is used to form an electron (\mathcal{L}_e) and non-electron ($\mathcal{L}_{\bar{e}}$) likelihood; these are combined into a likelihood ratio $\mathcal{R}_e = \mathcal{L}_e/(\mathcal{L}_e + \mathcal{L}_{\bar{e}})$ [12]. Applying a requirement on \mathcal{R}_e , electrons are selected with an efficiency and a misidentification rate of approximately 90% and 0.1%, respectively, in the kinematic region of interest. Muons are distinguished from other charged tracks by their range and hit profiles in the KLM. This information is utilized in a likelihood ratio approach [13] similar to the one used for the electron identification. Muons are selected with an efficiency and a misidentification rate of approximately 90% and 1%, respectively, in the kinematic region of interest. These requirements are reversed in order to produce a lepton veto for identifying pion candidates.

We select well-vertexed heavy neutrino candidates using dr , the distance of closest approach to the IP in the plane perpendicular to the beam axis for each track; $d\phi$, the angle between the momentum vector and decay vertex vector of the heavy neutrino candidate; and dz_{vtx} , the distance between the daughter tracks at their closest approach in the direction parallel to the beam. Requirements vary depending on the presence of SVD hits on the tracks and on the heavy neutrino candidate flight length. The signal lepton and pion are fit to a common vertex. Only candidates with $\chi_1^2/ndf < 16$, where χ_1^2 is the goodness of fit and ndf is the number of degrees of freedom, are accepted. A second vertex fit of the heavy neutrino candidate and the production lepton is performed with the vertex constrained to the IP; candidates with $\chi_2^2/ndf < 4$ are retained.

For combinatorial background, the daughter tracks of the heavy neutrino candidate often originate from the vicinity of the IP rather than the candidate’s decay vertex. In order to suppress this background, the difference between the radial coordinates of the closest associated hit in the SVD or CDC of either of the two daughter tracks to the IP (r_ℓ or r_π) and

the candidate's decay vertex (r_{vtx}) is calculated: $dr_{\text{fh}} = \min(r_\ell, r_\pi) - r_{\text{vtx}}$. This requirement is most effective for large r_{vtx} . The analysis requires $dr_{\text{fh}} > -2$ cm for $r_{\text{vtx}} > 6$ cm.

For the ‘‘small mass’’ ($M(\nu_h) < 2 \text{ GeV}/c^2$) analysis, $B \rightarrow D^{(*)} \ell \nu_h$ events are selected using the recoil mass against the $\ell\ell\pi$ system. This requirement is related to the kinematics of the decay under study. For $B \rightarrow X \ell \nu_h \rightarrow X \ell \ell \pi$ decays, the mass of X can be obtained from $M_X^2 = (E_{\text{CM}} - E_{\ell\ell\pi})^2 - P_{\ell\ell\pi}^2 - P_B^2 - 2\vec{P}_{\ell\ell\pi} \cdot \vec{P}_B$, where E_{CM} and P_B are the B meson center-of-mass (CM) energy and momentum and $E_{\ell\ell\pi}$ and $P_{\ell\ell\pi}$ are the CM energy and momentum of the $\ell\ell\pi$ system. The last term in this equation cannot be calculated as the B direction remains unknown, so we redefine the recoil mass as $M_X^2 \equiv (E_{\text{CM}} - E_{\ell\ell\pi})^2 - P_{\ell\ell\pi}^2 - P_B^2$. For events with $X = D^{(*)}$, the M_X distribution has overlapping peaks around the masses of the D and D^* , while for background events the recoil mass has a broader distribution. Events with $1.4 \text{ GeV}/c^2 < M_X < 2.4 \text{ GeV}/c^2$ are selected as candidates.

To reject protons from the decays of long-lived baryons, we impose a loose proton veto for the pion candidate. For each track, the likelihood values \mathcal{L}_p and \mathcal{L}_K of the proton and kaon hypotheses, respectively, are determined from the information provided by the hadron identification system (CDC, ACC, and TOF). A track is identified as a proton if $\mathcal{L}_p/(\mathcal{L}_p + \mathcal{L}_K) > 0.99$. Background events, rejected by the veto, are concentrated at heavy neutrino masses below $2 \text{ GeV}/c^2$ and thus this veto is applied in the ‘‘small mass’’ analysis only.

Using the requirements described above, the number of background events is reduced by a factor of $\sim 10^6$ to a handful of events, as shown in Fig. 3. Their summary is shown in Table I. The five event types in the Table are: I: both neutrino daughter tracks have recorded hits in SVD, II: one of the neutrino daughter tracks has recorded hits in SVD, III: none of the neutrino daughter tracks have recorded hits in SVD, and $r_{\text{vtx}} < 12$ cm, IV: no SVD hits and $12 \text{ cm} < r_{\text{vtx}} < 30$ cm, V: no SVD hits and decay radius exceeds $r_{\text{vtx}} > 30$ cm. The reconstruction efficiency for signal events does not depend significantly on the reconstruction mode ($e\ell\pi$, $\mu\mu\pi$ or $e\mu\pi$), but does depend strongly on the heavy neutrino mass. For a given mass, the efficiency also depends on the B -meson decay mode in which the heavy neutrino is produced. Efficiency distributions, including reconstruction efficiency, for different production modes are shown in Fig. 2. Efficiency of the requirements alone does not depend much on mass or production mode. Table I shows requirements efficiency for $D\ell\nu_h$ mode and $M(\nu_h) = 2 \text{ GeV}/c^2$. The efficiency drops with the radius r_{vtx} of the decay vertex from the beam axis. The effective range of neutrino reconstruction extends to $r_{\text{vtx}} \simeq 60$ cm.

If the heavy neutrino lifetime is long enough, then the number of neutrinos detected in the Belle detector is (in units where $\hbar = c = 1$)

$$\begin{aligned} n(\nu_h) &= 2N_{BB} \mathcal{B}(B \rightarrow X \ell \nu_h) \mathcal{B}(\nu_h \rightarrow \ell \pi) \int \varepsilon(R) \frac{m\Gamma}{p} \exp\left(-\frac{mR\Gamma}{p}\right) dR \\ &\simeq |U_\alpha|^2 |U_\beta|^2 2N_{BB} f_1(m) f_2(m) \frac{m}{p} \int \varepsilon(R) dR, \end{aligned} \quad (2)$$

where N_{BB} is the number of $B\bar{B}$ pairs, $\mathcal{B}(B \rightarrow X \ell \nu_h)$ is the total branching fraction for ν_h production, $\mathcal{B}(\nu_h \rightarrow \ell \pi)$ is the branching fraction of the reconstructed decay, $\varepsilon(R)$ is the reconstruction efficiency of the ν_h decaying at a distance R from the IP and m , p and Γ are the mass, momentum and full width of the heavy neutrino, respectively. Additionally, to factor out the $|U|^2$ dependence, we define $|U_\alpha|^2 f_1(m) \equiv \mathcal{B}(B \rightarrow X \ell \nu_h)$ and $|U_\beta|^2 f_2(m) \equiv \Gamma(\nu_h \rightarrow$

TABLE I. Summary of requirements, their background suppression efficiency, efficiency for signal events and systematic uncertainties.

Requirement	Applied to	Supp. eff., %	Signal eff., %	Syst. error, %
$\chi_1^2/ndf < 16$	All	35	99	2.9
$\chi_2^2/ndf < 4$	All	27	85	10.1
$\mathcal{R}_e(\ell_1) > 0.9$	All	40	45	2.2
$\mathcal{R}_\mu(\ell_1) > 0.99$	All	17	35	4.9
$\mathcal{R}_e(\ell_2) > 0.9$	All	38	53	3.0
$\mathcal{R}_\mu(\ell_2) > 0.9$	All	25	38	3.1
Lepton veto	All	86	99	1.8
$d\phi < 0.03$ cm	Type I	39	95	} 5.8
$d\phi < 0.03$ cm	Type II	5	80	
$d\phi < 0.04$ cm	Type III	11	85	
$d\phi < 0.09$ cm	Type IV	66	96	
$d\phi < 0.15$ cm	Type V	51	94	
$dr > 0.09$ cm	Type I	5	97	} 3.7
$dr > 0.1$ cm	Type II	7	98	
$dr > 3$ cm	Type III	1	79	
$dr > 3$ cm	Type IV	10	94	
$dr > 5$ cm	Type V	42	95	
$dz_{\text{vtx}} < 0.4$ cm	Type I	37	94	} 10.0
$dz_{\text{vtx}} < 0.4$ cm	Type II	17	74	
$dz_{\text{vtx}} < 0.5$ cm	Type III	21	75	
$dz_{\text{vtx}} < 0.9$ cm	Type IV	36	80	
$dz_{\text{vtx}} < 2$ cm	Type V	68	83	
$dr_{\text{fb}} > -2$ cm	$r_{\text{vtx}} > 6$ cm	32	84	2.9
Recoil mass	Small mass	24	99	4.1
Proton veto	Small mass	94	97	1.6

$\ell\pi) = \mathcal{B}(\nu_h \rightarrow \ell\pi)\Gamma$, where α and β denote the flavor of the charged lepton produced in the B and ν_h decay, respectively. The exponent in the integrand of Eqn. (2) is approximated by unity. An error introduced by this approximation is small and is negligible when the flight length is long enough (for $|U|^2 \lesssim 10^{-3}$). Integration is performed over the full volume used to reconstruct the heavy neutrino vertex, which depends on the reconstruction requirements. The expressions for $\mathcal{B}(B \rightarrow X\ell\nu_h)$ and $\Gamma(\nu_h \rightarrow \ell\pi)$ are taken from Ref. [11] and require only very general assumptions (i.e., they are not specific to ν MSM).

The calculated total branching fractions for heavy neutrino production $\mathcal{B}(B \rightarrow X\ell\nu_h)$ for the “small mass” and “large mass” analyses correspond to

$$\mathcal{B}(B \rightarrow X\ell\nu_h)_{\text{small mass}} = \mathcal{B}(B \rightarrow D\ell\nu_h) + \mathcal{B}(B \rightarrow D^*\ell\nu_h) \quad (3)$$

and

$$\mathcal{B}(B \rightarrow X\ell\nu_h)_{\text{large mass}} = \sum_i \mathcal{B}(B \rightarrow X_i\ell\nu_h), \quad (4)$$

respectively, where the summation is done over D , D^* , π , ρ , η , η' , ω , ϕ and ‘nothing.’ These are not exact expressions but rather estimates of lower bounds on $\mathcal{B}(B \rightarrow X\ell\nu_h)$, which lead to conservative upper limits on $|U|^2$.

The systematic uncertainty of each of the event selection criteria is estimated from the difference in the efficiencies obtained in data and MC. A summary of all systematic uncertainties is presented in Table I. Since all particles used in the systematic uncertainty study decay relatively close to the IP compared to the expectation for a heavy neutrino, we require where possible that the decay vertices be farther than 4 cm from the IP in the transverse plane to put more weight on large decay lengths. To estimate the systematic uncertainty due to tracking, we compare the number of fully and partially reconstructed D^* decays in the decay chain $D^* \rightarrow D\pi^+$, $D \rightarrow K_S^0\pi\pi$, $K_S^0 \rightarrow \pi\pi$, where in the latter case one of the pions from the K_S^0 is explicitly left unreconstructed. To estimate the systematic uncertainty of the recoil mass requirement, we reconstruct $B \rightarrow DD_s^{(*)}$, $D \rightarrow K_S^0\pi$ events and study the mass recoiling against the D -meson. The D decay topology is similar to $\ell\nu_h$ here, and we treat the difference in recoil mass efficiency between data and MC as the systematic uncertainty of the recoil mass requirement. To estimate the systematic uncertainty of the electron identification, we reconstruct $\pi^0 \rightarrow \gamma\gamma$ events, where one of the photons converts into e^+e^- in the detector and one of these conversion particles is identified as an electron. The difference of the identification efficiency of the other daughter between data and MC is treated as a systematic uncertainty. For the muon identification, we perform a similar study with a $J/\psi \rightarrow \mu^+\mu^-$ sample. To estimate the systematic uncertainty of other reconstruction requirements, we apply these requirements to K_S^0 decays, which have a topology similar to heavy neutrino decays. Correlations between different systematic uncertainties are found to be small and are neglected. All systematic uncertainties are summed in quadrature, leading to total systematic uncertainties of 25.0% and 25.4% for the “small mass” and “large mass” regimes, respectively. The largest contributions to the systematic uncertainties are χ_2^2 (10.1%), dz_{vtx} (10.0%) and tracking of the heavy neutrino candidate daughter particles (8.7% per track, added linearly).

After all the event selection criteria were fixed from the MC study, the data were analyzed and the coupling constants $|U_e|^2$, $|U_\mu|^2$ and $|U_e||U_\mu|$ were obtained separately using the decay modes $e\ell\pi$, $\mu\mu\pi$ and $e\mu\pi + \mu e\pi$, respectively. Distributions of the heavy neutrino mass in generic MC and data are shown in Fig. 3. In agreement with MC expectations, only a few isolated events are observed and we set upper limits on $|U|^2$ according to Ref. [14], taking into account the systematic uncertainty calculated above. For non-empty bins and empty bins far from non-empty bins, we set Poisson upper limits, assuming small background, as suggested from the MC study. In the vicinity of non-empty bins, we use Gaussian fits to interpolate between empty and non-empty regions. The widths of the Gaussians are fixed from MC. We use bins of $3 \text{ MeV}/c^2$ width, since the mass resolution evolves from $\sim 3 \text{ MeV}/c^2$ at $M(\nu_h) = 1 \text{ GeV}/c^2$ to $\sim 12 \text{ MeV}/c^2$ at $M(\nu_h) = 4 \text{ GeV}/c^2$. The resulting upper limits at 90% CL on the number of events and coupling constants are shown in Fig. 4.

In conclusion, upper limits on the mixing of heavy right-handed neutrinos with the conventional SM left-handed neutrinos in the mass range $0.5 - 5.0 \text{ GeV}/c^2$ have been obtained. The maximum sensitivities are achieved around $2 \text{ GeV}/c^2$ and are 3.0×10^{-5} , 3.0×10^{-5} and 2.1×10^{-5} for $|U_e|^2$, $|U_\mu|^2$ and $|U_e||U_\mu|$, respectively. The corresponding upper limit for the

product branching fraction is $\mathcal{B}(B \rightarrow X\ell\nu_h) \times \mathcal{B}(\nu_h \rightarrow \ell\pi^+) < 7.2 \times 10^{-7}$ for $\ell = e$ or μ . A comparison with existing results for $|U_e|^2$ and $|U_\mu|^2$ is shown in Fig. 5.

We thank the KEKB group for the excellent operation of the accelerator; the KEK cryogenics group for the efficient operation of the solenoid; and the KEK computer group, the National Institute of Informatics, and the PNNL/EMSL computing group for valuable computing and SINET4 network support. We acknowledge support from the Ministry of Education, Culture, Sports, Science, and Technology (MEXT) of Japan, the Japan Society for the Promotion of Science (JSPS), and the Tau-Lepton Physics Research Center of Nagoya University; the Australian Research Council and the Australian Department of Industry, Innovation, Science and Research; the National Natural Science Foundation of China under contract No. 10575109, 10775142, 10875115 and 10825524; the Ministry of Education, Youth and Sports of the Czech Republic under contract No. LA10033 and MSM0021620859; the Department of Science and Technology of India; the Istituto Nazionale di Fisica Nucleare of Italy; the BK21 and WCU program of the Ministry Education Science and Technology, National Research Foundation of Korea Grant No. 2010-0021174, 2011-0029457, 2012-0008143, 2012R1A1A2008330, BRL program under NRF Grant No. KRF-2011-0020333, and GSDC of the Korea Institute of Science and Technology Information; the Polish Ministry of Science and Higher Education and the National Science Center; the Ministry of Education and Science of the Russian Federation and the Russian Federal Agency for Atomic Energy; the Slovenian Research Agency; the Swiss National Science Foundation; the National Science Council and the Ministry of Education of Taiwan; and the U.S. Department of Energy and the National Science Foundation. This work is supported by a Grant-in-Aid from MEXT for Science Research in a Priority Area (“New Development of Flavor Physics”), and from JSPS for Creative Scientific Research (“Evolution of Tau-lepton Physics”).

-
- [1] J. Beringer *et al.* (Particle Data Group), Phys. Rev. D **86**, 010001 (2012).
 - [2] P. Minkowski, Phys. Lett. B **67**, 421 (1977); T. Yanagida, in *Proc. of the Workshop on Grand Unified Theory and Baryon Number of the Universe, KEK, Japan, 1979* (KEK Report No. 79-18, 1979), p. 95; M. Gell-Mann, P. Ramond and R. Slansky, (1980), Print-80-0576 (CERN); R.N. Mohapatra and G. Senjanovic, Phys. Rev. Lett. **44**, 912 (1980).
 - [3] T. Asaka, S. Blanchet and M. Shaposhnikov, Phys. Lett. B **631**, 151 (2005); T. Asaka and M. Shaposhnikov, Phys. Lett. B **620**, 17 (2005).
 - [4] J.A. Harvey, P. Ramond and D.B. Reiss, Nucl. Phys. B **199**, 223 (1982); S. Dimopoulos, L.J. Hall and S. Raby, Phys. Rev. Lett. **68**, 1984 (1992); L.J. Hall and S. Raby, Phys. Rev. D **51**, 6524 (1995).
 - [5] I. Dorsner and P. Fileviez Perez, Nucl. Phys. B **723**, 53 (2005).
 - [6] A. Zee, Phys. Lett. B **93**, 389 (1980) [Erratum - *ibid.* **B95**, 461 (1980)]; A. Zee, Phys. Lett. B **161**, 141 (1985); E. Ma and U. Sarkar, Phys. Rev. Lett. **80**, 5716 (1998).
 - [7] A. Atre, T. Han, S. Pascoli and B. Zhang, JHEP **0905**, 030 (2009).
 - [8] S. Kurokawa and E. Kikutani, Nucl. Instr. and Meth. A **499**, 1 (2003), and other papers included in this volume.
 - [9] A. Abashian *et al.* (Belle Collaboration), Nucl. Instr. and Meth. A **479**, 117 (2002).
 - [10] D.J. Lange, Nucl. Instr. and Meth. A **462**, 152 (2001); EvtGen — A Monte Carlo Generator for B-physics, A. Ryd *et al.*, 14/3/2002.

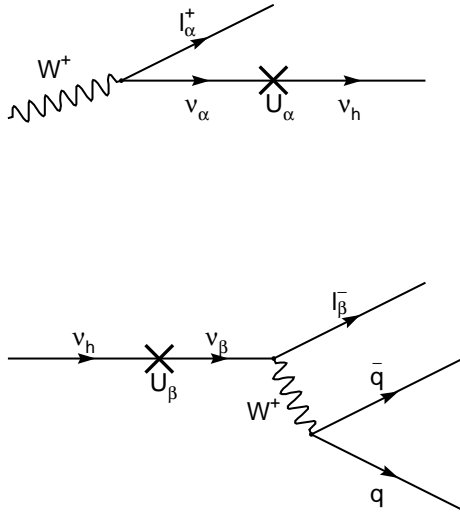


FIG. 1. Heavy neutrino production (*top*) and decay (*bottom*) diagrams.

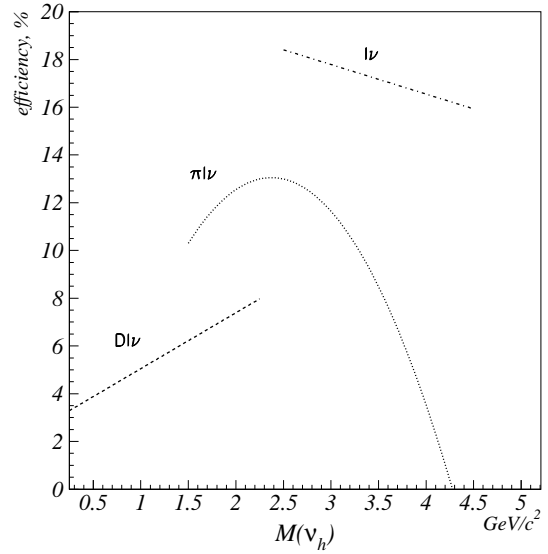


FIG. 2. Efficiency distributions for different production modes.

- [11] D. Gorbunov and M. Shaposhnikov, JHEP **0710**, 015 (2007).
- [12] K. Hanagaki *et al.*, Nucl. Inst. and Meth. A **485**, 490 (2002).
- [13] A. Abashian *et al.*, Nucl. Inst. and Meth. A **491**, 69 (2002).
- [14] G.J. Feldman and R.D. Cousins, Phys. Rev. D **57**, 3873 (1998).
- [15] F. Bergsma *et al.* (CHARM Collaboration), Phys. Lett. B **166**, 473 (1986).
- [16] P. Vilain *et al.* (CHARM II Collaboration), Phys. Lett. B **343**, 453 (1995); P. Vilain *et al.* (CHARM II Collaboration), Phys. Lett. B **351**, 387 (1995).
- [17] P. Abreu *et al.* (DELPHI Collaboration), Z. Phys. C **74**, 57 (1997) [Erratum-ibid. C **75**, 580 (1997)].
- [18] A. Vaitaitis *et al.* (NuTeV Collaboration), Phys. Rev. Lett. **83**, 4943 (1999).
- [19] A.M. Cooper-Sarkar *et al.* (BEBC-WA66 Collaboration), Phys. Lett. B **160**, 207 (1985).
- [20] J. Badier *et al.* (NA3 Collaboration), Z. Phys. C **31**, 21 (1986).

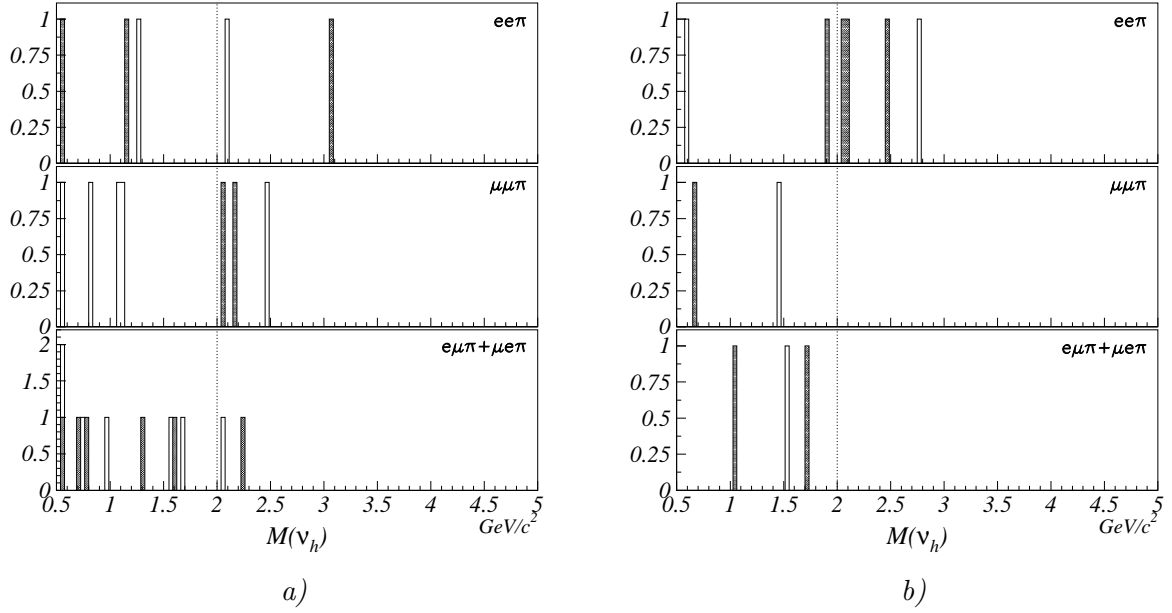


FIG. 3. Distributions of $M(\nu_h)$ for $ee\pi$, $\mu\mu\pi$ and $e\mu\pi + \mu e\pi$ reconstruction modes in generic MC (unscaled) (a), and data (b). The dotted line shows the boundary between the “small mass” and “large mass” methods. The filled (black) histograms are for candidates with opposite-charge leptons, while the open (white) histograms are for candidates with same-charge leptons.

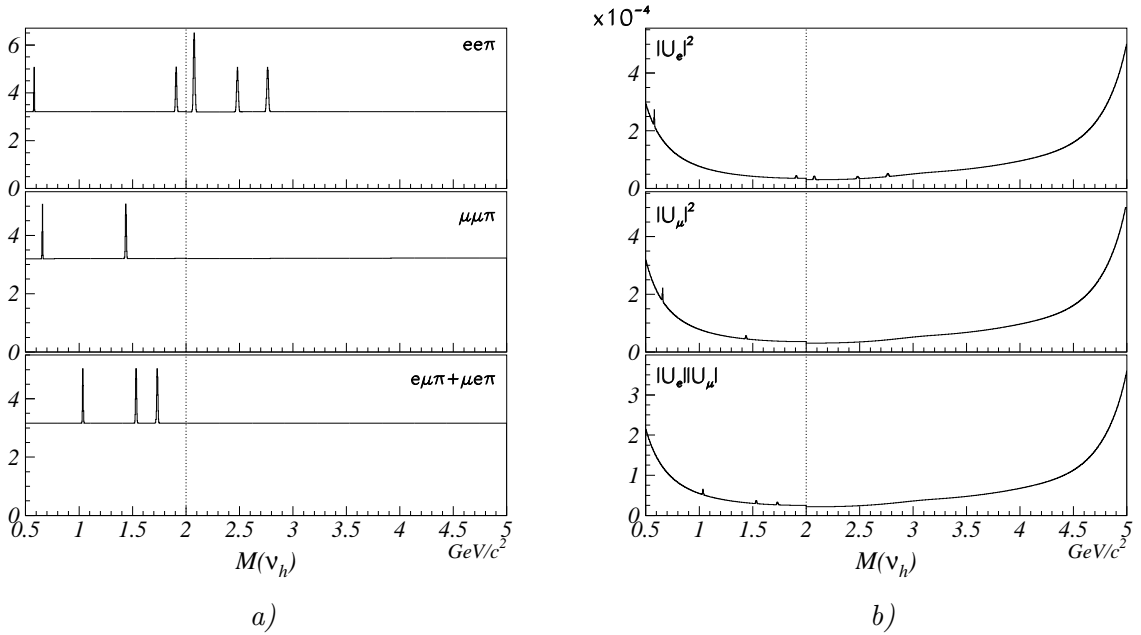


FIG. 4. Upper limits at 90% CL on the number of signal events (a) and $|U_e|^2$, $|U_\mu|^2$ and $|U_e||U_\mu|$ (b). The dotted line shows the boundary between the “small mass” and “large mass” methods.

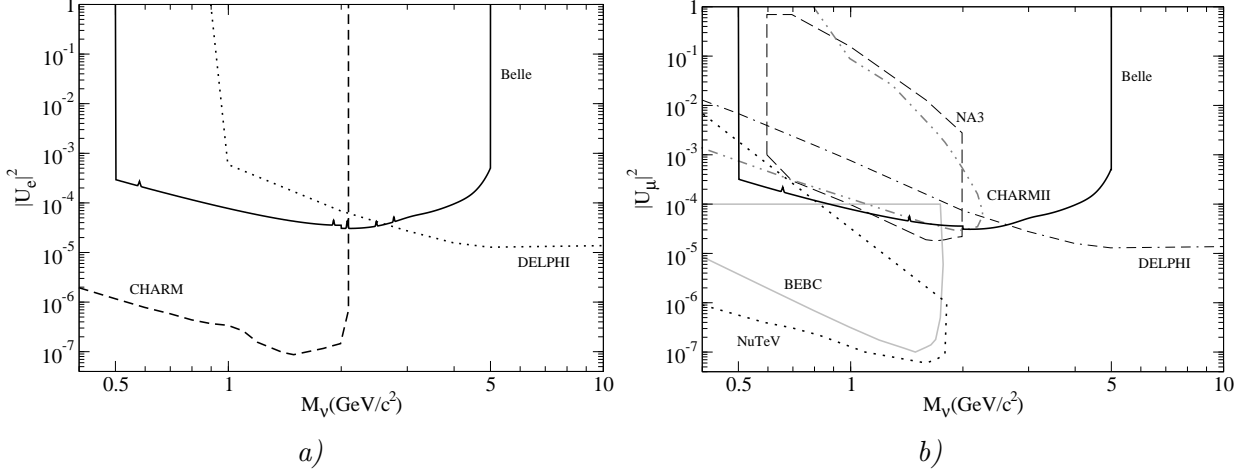


FIG. 5. Comparison of the obtained upper limits for $|U_e|^2$ (a) and $|U_\mu|^2$ (b) with existing experimental results from CHARM [15], CHARMII [16], DELPHI [17], NuTeV [18], BEBC [19] and NA3 [20].

Erratum: Search for heavy neutrinos at Belle [Phys. Rev. D **87**, 071102(R) (2013)]

D. Liventsev^{1,2}

(The Belle Collaboration)

¹*CNP, Virginia Polytechnic Institute and State University, Blacksburg, Virginia 24061*

²*High Energy Accelerator Research Organization (KEK), Tsukuba 305-0801*

(Dated: October 29, 2018)

The number of neutrinos detected in the Belle detector is (Eqn. (2) of Ref. [1]):

$$n(\nu_h) = 2N_{BB} \mathcal{B}(B \rightarrow \nu_h) \mathcal{B}(\nu_h \rightarrow \ell\pi) \int \frac{m\Gamma}{p} \exp\left(-\frac{m\Gamma R}{p}\right) \varepsilon(R) dR \quad (1)$$

$$= |U_\alpha|^2 |U_\beta|^2 2N_{BB} f_1(m) f_2(m) \frac{m}{p} \int \exp\left(-\frac{m\Gamma R}{p}\right) \varepsilon(R) dR \quad (2)$$

where N_{BB} is the number of $B\bar{B}$ pairs, $\mathcal{B}(B \rightarrow \nu_h)$ is the total branching fraction for ν_h production, $\mathcal{B}(\nu_h \rightarrow \ell\pi)$ is the branching fraction of the reconstructed decay, $\varepsilon(R)$ is the reconstruction efficiency of the ν_h decaying at a distance R from the interaction point, m , p and Γ are the mass, momentum and full width of the heavy neutrino, respectively. Integration is performed over the full volume used to reconstruct the heavy neutrino vertex, which depends on reconstruction requirements. Addi-

tionally, to factor out the $|U|^2$ dependence, we define $|U_\alpha|^2 f_1(m) \equiv \mathcal{B}(B \rightarrow \nu_h)$ and $|U_\beta|^2 f_2(m) \equiv \Gamma(\nu_h \rightarrow \ell\pi) = \mathcal{B}(\nu_h \rightarrow \ell\pi)\Gamma$, where α and β denote the flavor of the charged lepton produced in the B and ν_h decays, respectively.

In the original paper [1], the exponent in the integrand was approximated by unity under the assumption that Γ is small and the flight length is sufficiently long:

$$n(\nu_h) \simeq |U_\alpha|^2 |U_\beta|^2 2N_{BB} f_1(m) f_2(m) \frac{m}{p} \int \varepsilon(R) dR. \quad (3)$$

Here, the momentum of the heavy neutrino was kept constant.

The assumption of a long flight length is valid only for a small neutrino mass. However, since the partial decay widths approximately increase with mass as m^3 to m^5 depending on the final state [2], at higher masses this approximation introduces a significant overestimation of the upper limit on $|U|^2$. Moreover, at large masses there is also an upper bound of the excluded region since, for some values of the coupling constant, the flight length is so small that the event is rejected by the selection criteria. Therefore, we recalculate the upper limits on

$|U|^2$ taking into account the exponent in Eqn. 2 and the actual neutrino momentum. The full neutrino width Γ is calculated as the sum of partial widths from Ref. [2]. Since we do not know the relation among the different U_α we assume $|U|^2 = |U_\alpha||U_\beta|$ in the calculation of Γ . To obtain the upper limit on the coupling constants, we solve the Eqn. 2 for the variable $|U|^2$.

The updated versions of Figs. 4b and 5 in the original paper with the new calculation are shown here as Figs. 1 and 2, respectively.

We thank Brian Shuve and Michael Peskin for pointing out the issue.

[1] D. Liventsev *et al.* (Belle collaboration), Phys. Rev. D. **87**, 071102 (2013).

[2] D. Gorbunov and M. Shaposhnikov, JHEP **0710**, (2007) 015 [arXiv:0705.1729 [hep-ph]].

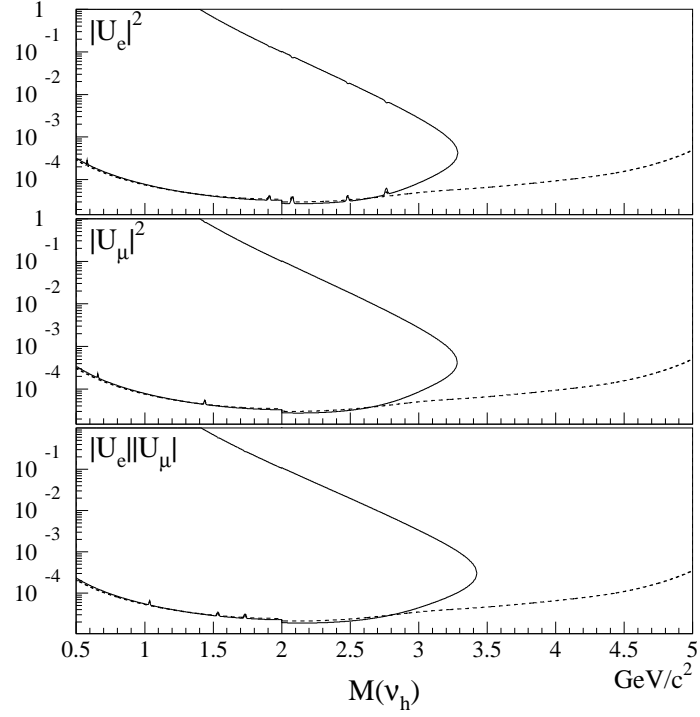


FIG. 1. Upper limits at 90% CL on the $|U_e|^2$, $|U_\mu|^2$ and $|U_e||U_\mu|$. The solid line shows the correct exclusion region; the dashed line shows the one from the original paper.

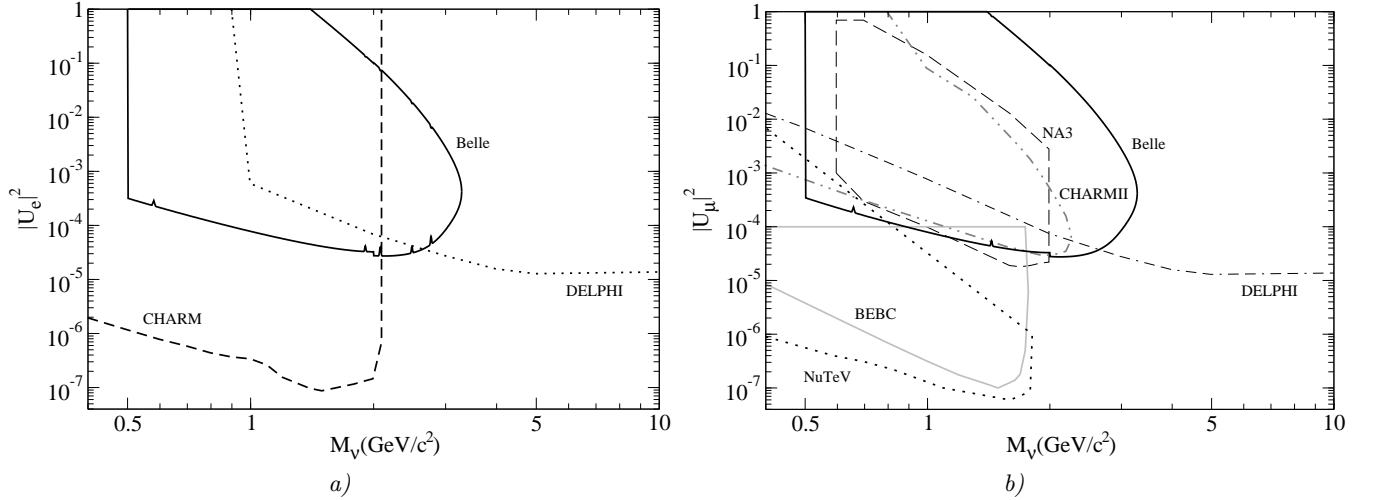


FIG. 2. Comparison of the obtained upper limits for $|U_e|^2$ (a) and $|U_\mu|^2$ (b) with existing experimental results from CHARM, CHARMII, DELPHI, NuTeV, BEBC and NA3.